REPORT DOCUMENTATION PAGE

AFRL-SR-BL-TR-98- 0433 JANG

1. AGENCY USE ONLY (Leave blank)	2. REPORT DATE	3. REPORT TYPE AND DATES COVERED
	27 April 1998	Final Technical Report 01 Nov. 93 - 31 Oct. 97

4. TITLE AND SUBTITLE
Broadband Signal Enhancement of Seismic Array Data: Application to Long-Period Surface Waves & High Frequency Wavefields

5. FUNDING NUMBERS
Contract # F49620-94-1-0037

6. AUTHOR(S)
Frank L. Vernon
Robert J. Mellors
David J. Thomson*

7. PERFORMING ORGANIZATION NAME(S) AND ADDRESS(ES)
The Regents of the University of California
Scripps Institution of Oceanography
IGPP 0225, 9500 Gilman Drive
La Jolla, California 92093-0225

*Bell Labs
Lucent Technologies
Murray Hill, New Jersey

8. PERFORMING ORGANIZATION REPORT NUMBER

9. SPONSORING/MONITORING AGENCY NAME(S) AND ADDRESS(ES)
AFOSR
110 Duncan Avenue Room B115
Bolling AFB DC 20332-8080
Prgram Manager: Dr. Stanley K. Dickinson/NM

NL

10. SPONSORING /MONITORING AGENCY REPORT NUMBER

11. SUPPLEMENTARY NOTES

12a. DISTRIBUTION/AVAILABILITY STATEMENT
Approved for public release, distribution unlimited

12b. DISTRIBUTION CODE

13. ABSTRACT *(Maximum 200 words)*

We demonstrated the use of "dual-frequency" coherence in detecting and characterizing seismic surface waves. Using a multitaper method, we calculated the coherence between different frequencies of one or multiple signals. We tested the algorithm both on a variety of synthetic signals and on broadband seismic data. Dispersive waves such as seismic surface waves are easily identified and we showed that the method is robust in the presence of noise. Phase relationships between different frequencies can be extracted, allowing reconstruction of the original phase function. "Dual-frequency" coherence is useful in identifying overtones and frequency shifts between signals, features which are undetectable by standard coherence measures. We constructed a filter to extract only the coherent frequencies from a waveform and showed that it significantly increases the signal-noise-ratio for dispersive waveforms.

14. SUBJECT TERMS
"dual-frequency"
seismic surface waves

15. NUMBER OF PAGES
31

16. PRICE CODE

17. SECURITY CLASSIFICATION OF REPORT	18. SECURITY CLASSIFICATION OF THIS PAGE	19. SECURITY CLASSIFICATION OF ABSTRACT	20. LIMITATION OF ABSTRACT
Unclassified	Unclassified	Unclassified	SAR

NSN 7540-01-280-5500

Standard Form 298 (Rev 2-89)
Prescribed by ANSI Std. 239-18
298-102

BROADBAND SIGNAL ENHANCEMENT OF SEISMIC ARRAY DATA: APPLICATION TO LONG-PERIOD SURFACE WAVES AND HIGH-FREQUENCY WAVEFIELDS

Frank L. Vernon
Robert J. Mellors
David J. Thomson*

University of California, San Diego
Scripps Institution of Oceanography
Cecil H. and Ida M. Green Institute of Geophysics and Planetary Physics
9500 Gilman Drive
La Jolla CA 92093-0255

Bell Labs*
Lucent Technologies
Murray Hill, New Jersey

April 28, 1998

Final Technical Report
November 1, 1993 - October 31, 1997

Contract No. F49620-94-1-0037

Abstract

We demonstrate the use of "dual-frequency" coherence in detecting and characterizing seismic surface waves. Using a multitaper method, we calculate the coherence between different frequencies of one or multiple signals. We test the algorithm both on a variety of synthetic signals and on broadband seismic data. Dispersive waves such as seismic surface waves are easily identified and we show that the method is robust in the presence of noise. Phase relationships between different frequencies can be extracted, allowing reconstruction of the original phase function. "Dual-frequency" coherence is useful in identifying overtones and frequency shifts between signals, features which are undetectable by standard coherence measures. We construct a filter to extract only the coherent frequencies from a waveform and show that it significantly increases the signal-noise-ratio for dispersive waveforms.

Contents

List of Figures

1 Summary

We demonstrate the use of "dual-frequency" coherence in detecting and characterizing seismic surface waves. Using a multitaper method, we calculate the coherence between different frequencies of one or multiple signals. We test the algorithm both on a variety of synthetic signals and on broadband seismic data. Dispersive waves such as seismic surface waves are easily identified and we show that the method is robust in the presence of noise. Phase relationships between different frequencies can be extracted, allowing reconstruction of the original phase function. "Dual-frequency" coherence is useful in identifying overtones and frequency shifts between signals, features which are undetectable by standard coherence measures. We construct a filter to extract only the coherent frequencies from a waveform and show that it significantly increases the signal-noise-ratio for dispersive waveforms.

2 Introduction

We demonstrate the use of "dual-frequency" coherence in characterizing, filtering and detecting seismic surface waves. Standard coherency has long been used to evaluate the similarity between time series (e.g. *Tick*, 1966; *Foster and Guinzy*, 1967; *Hinich and Clay*, 1968; *Vernon et al.*, 1991; *Hough and Field*, 1996) and is an estimate of the correlation coefficient between the Fourier components of two time series at a given frequency (*Priestley*, 1981). In contrast, "dual-frequency" coherence is an estimate of the correlation coef-

ficient between Fourier components for all possible pairs of frequencies. *Lòeve* (1945) first defined dual-frequency spectra and described them in his 1963 book (*Lòeve*, 1963). Because experience has shown that it is more convenient to use coherences than cross-spectra in the stationary case, we convert the dual-frequency spectra to dual-frequency coherences.

We use the definition of *Thomson (1982)* to calculate the dual-coherence between different frequencies of the same or different signals. Coherency between different frequencies is high when the frequency components (amplitude and phase) of the two signals are correlated. We show in this paper that coherencies between different frequencies exist in seismic surface waves and that this coherence is useful in signal detection as well as in the identification of such features as multi-pathing and higher modes.

An important implication of correlation between different frequencies is that it implies that the time series are non-stationary, either individually or jointly. Most methods of spectral estimation assume that the data is stationary; however, much real data, especially seismic data, is not stationary, at least locally. This non-stationarity, if not accounted for, will adversely affect the reliability of the resulting spectral estimate (*Thomson*, 1993). Because spectral estimates are essential in many surface wave studies, it is important to develop methods capable of assessing and handling non-stationary signals. Dual-frequency coherency provides one method of evaluating the amount of non-stationarity.

The dual-frequency coherence algorithm uses the multiple-taper approach

of *Thomson* (1982) (also see *Lanzerotti et al.*, 1986; *Vernon et al.*, 1991; *Percival and Walden*, 1993; *Kuo et al.*, 1990; *Park et al.*, 1987) to calculate the coherency. The multiple tapers supply the smoothing needed for the cross-spectral estimate, in contrast to the time-averaging commonly used in other coherency estimates (e.g. Welch's method [*Percival and Walden, 1993]).*

The strength of dual-frequency coherency is that it can identify frequency relationships that are invisible to standard coherency estimates (*Vernon et al.*, 1995; *Mellors et al.*, 1996). In particular, features such as harmonics and non-linear frequency translations (such as those produced by Doppler shifts) are immediately identifiable. *Park et al.* (1993) used dual-frequency coherence to identify harmonics in times series of climate data. Dispersive signals, in which neighboring frequency components possess similar amplitude and phase, are also easily discerned. Consequently, seismic surface waves, which are highly dispersive, can be easily and effectively analyzed by this method.

We extend the algorithm to compute coherency as a function of time and frequency ("coherogram") and show that this is useful in identifying specific phases in the seismograms. Phase relationships between frequencies can be extracted suggesting that the method may have potential to determine dispersion curves. Finally, we construct a filter to extract the coherent frequencies by deleting non-coherent frequencies and converting back into the time domain. This filtering provides a simple and effective way to enhance the signal-to-noise ratio for use in a detection scheme. This filtering does

not assume any *a priori* knowledge of the signal (other than the fact it is dispersive to some degree).

We demonstrate our technique using a variety of synthetic waveforms to illustrate the method and then we apply it to seismic data.

3 Method

The use of multitaper spectral estimates to calculate coherences was first suggested by *Thomson* (1982). Multitaper spectral estimates combine weighted FFTs from a number of differently tapered versions of a given signal to yield a single spectral estimate.

Specifically, given $x(t)$ with N data samples and a chosen time-bandwidth product W, compute the eigencoefficients $y_k(f)$:

$$y_k(f) = \sum_{t=0}^{N-1} v_t^{(k)}(N,W) x_t e^{-i2\pi ft} \tag{1}$$

for $k = 0, 1...(2NW-1)$ where $v_t^{(k)}(N,W)$ is the k^{th} Slepian sequence. The tapers are based on the prolate spheroidal series developed by *Slepian* (1978, 1983) and are optimized to minimize leakage from outside the desired band. Individual tapers are orthogonal, and collectively define the time and bandwidth. The orthogonal tapers provide approximately independent estimates of the spectra, which can be used to construct error estimates *(Thomson and Chave, 1991)*.

The weights are adaptively determined using an iterative process for each

time series. The resulting estimate, $S(f)$ is a combination of all these factors:

$$S(f) = \frac{A}{K} \frac{\sum_{k=0}^{K-1} \lambda_k d_k^2(f) |y_k(f)|^2}{\sum_{k=0}^{K-1} d_k^2(f)} \tag{2}$$

where d_k are the weights of the each spectral estimate, λ_k are the eigenvalues associated with each taper, and y_k are the discrete Fourier transforms of the tapered data. A is determined using

$$A = \sum_{k=0}^{K-1} \lambda_k^{-1} \tag{3}$$

and K is the number of tapers. Multi-taper estimates are especially effective for time series which are either short or have a large dynamic range. The adaptive weighting gives minimum errors in a stationary sequence and the double orthogonality of the Slepian functions implies near optimality in non-stationary data.

A cross-spectra $S_{ij}(f)$ between two time series i and j is calculated using:

$$S_{ij}(f) = \frac{A}{K} \frac{\sum_{k=0}^{K-1} \lambda_k d_k^i(f) (y_k^i(f))^* d_k^j(f) (y_k^j(f))}{[\sum_{k=0}^{K-1} d_k^i(f)^2]^{\frac{1}{2}} [\sum_{k=0}^{K-1} d_k^j(f)^2]^{\frac{1}{2}}} \tag{4}$$

Standard coherence (magnitude squared) is therefore:

$$\gamma_{ij}^2(f) = \frac{|S_{ij}(f)|^2}{S_{ii}(f) S_{jj}(f)} \tag{5}$$

This yields a coherence estimate between two different signals at a given frequency (e.g. *Vernon et al.*, 1991). If only one taper ($K = 1$) is used, the coherence estimate is unity. The additional tapers provide a smoothing effect that negates the need for the time-frequency averaging commonly

used in standard coherence estimates. To calculate the cross-spectra between different frequencies we modify equation (4) to:

$$S_{ij}(f_1, f_2) = \frac{A}{K} \frac{\sum_{k=0}^{K-1} \lambda_k d_k^i(f_1)(y_k^i(f_1))^* d_k^j(f_2)(y_k^j(f_2))}{[\sum_{k=0}^{K-1} d_k^i(f_1)^2]^{\frac{1}{2}} [\sum_{k=0}^{K-1} d_k^j(f_2)^2]^{\frac{1}{2}}} \tag{6}$$

Consequently, dual-frequency coherence between two different frequencies f_1 and f_2 is:

$$\gamma_{ij}^2(f_1, f_2) = \frac{|S_{ij}(f_1, f_2)|^2}{S_{ii}(f_1) S_{jj}(f_2)} \tag{7}$$

The coherence is calculated not only between two signals, but also between different frequencies. If $f_1 = f_2$, the definition reduces to equation (5). An important feature of this definition is that the auto-dual-frequency coherence can be calculated, i.e. the dual-frequency coherence of a single signal with itself. The result is unity where $f_1 = f_2$ but yields a value between 1 and 0 elsewhere, which indicates the amount of coherence between different frequencies. Different frequencies are coherent if their amplitude and phase is similar. In a sense, dual-frequency coherence resembles a frequency domain cross-correlation. For a dispersive signal, coherence between neighboring frequencies is high.

For the rest of the paper, unless specified otherwise, when we refer to coherency we mean dual-frequency coherency between different series and auto-coherency is coherence between two frequency band components of the same signal.

4 Results and Discussion

Tests of the algorithm on simple synthetic signals illustrate the method. For all plots in this paper we use 12 tapers (K = 12) and a time-bandwidth product of 6.5. Figure 1 shows the auto-coherence of pseudo-random numbers $r(t)$ generated by Matlab *(Matlab*, 1994) and of a sweep (chirp) signal with $\sigma = 0.1$:

$$f(t) = 100\sin(2\pi t(f_a + \frac{(f_b - f_a)i}{600})) + \sigma r(t) \qquad 0 \leq t \leq 600 \qquad (8)$$

with $f_a = 0.0$ and $f_b = 0.075$. In both these cases we show the auto coherence. The coherence plot of the random noise shows a thin diagonal line, demonstrating that the signal is coherent with itself at the a given frequency, but shows low coherence between different frequencies. For random noise, different frequencies are uncorrelated and consequently the coherence depends on the degrees of freedom and therefore on K. In this case, the mean off-diagonal coherence is 0.0828. A diagonal line is evident for the sweep signal but it is wider, demonstrating that adjacent frequencies are highly coherent, as is expected for a sweep signal and also is a consequence of the ambiguity function. Further away from the main diagonal the coherence is low. At these frequency combinations the individual frequencies possess high power but the cross-spectra is low, creating a low coherence. At the ends of the sweep frequencies high coherence is observed but the power of the signal is low and consequently the coherence at these frequencies is highly sensitive to changes in noise level.

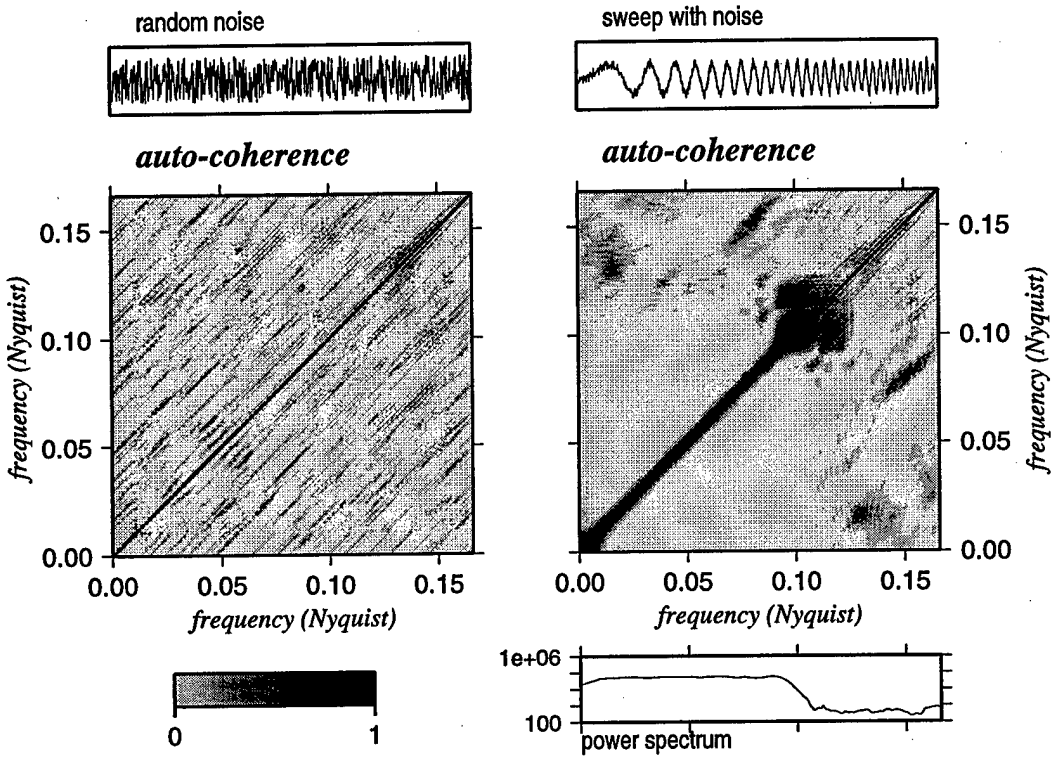

Figure 1: Double-frequency coherence of random noise (left) and a simple sweep signal (right). Each shaded matrix represents the coherence of a signal with itself calculated between all possible frequency combinations. Shading represents coherency from 0.0 to 1.0, with black indicating high coherency. The scale is in fractions of the Nyquist frequency. Only part of the full matrix is shown. The power spectrum of the sweep is shown below and is plotted on the same frequency scale.

The complex representation of the coherence also yields a phase ϕ using the full complex form of the estimate (without the absolute values shown in equation (5)). The phase is the phase difference between the two frequencies, as the cross spectra multiplies one complex frequency multiplied by the conjugate of the other. The variance of the phase is inversely related to the coherence and contains useful information only where the frequencies are highly coherent. The phase plot of the auto-coherence shows a center diagonal with $\phi = 0$. The neighboring diagonal represents the (wrapped) phase difference between frequencies separated by one Rayleigh resolution $f_2 = f_1 + \frac{1}{T}$. Reconstructing the original phase function is straightforward if the change in phase is not too large and the coherence is high. It is only necessary to unwrap and integrate the first off-diagonal. The resulting phase function will differ from the phase as determined by a direct FFT. Figure 2 shows the high correspondence between the phase measured using dual-frequency coherence and the known phase for a sweep signal.

A powerful feature of the dual-frequency coherence algorithm is the ability to identify relationships between different frequency components that are invisible to standard coherence estimates. Figure 3 shows two different sweep signals compared using dual-frequency coherence. One sweep signal is a frequency translated version of the other as might be caused by a Doppler shift or by two differing dispersion paths. We use the same function as before but with $f_b = 0.075$ for the first sweep and $f_b = 0.050$ for the second sweep. The dual-frequency coherence plot clearly shows the relationship between

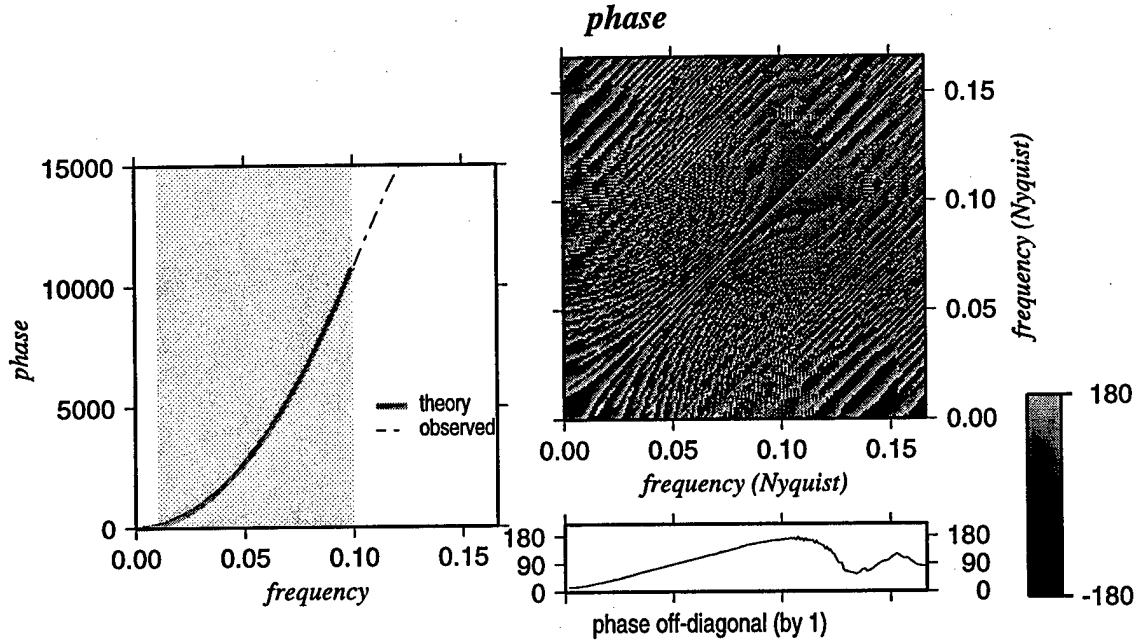

Figure 2: (left) Comparison of the phase derived using dual-frequency coherence (solid line) and the theoretical phase (dashed line). The shaded area represents the frequencies of high coherence. (right) The full phase matrix showing the difference in phase between the frequency components for the sweep signal shown in Figure 1. The lower plot shows the first off-diagonal of the matrix after unwrapping. Integration of the first off-diagonal yields the phase function shown in the plot at left.

the two signals. The signals are clearly coherent but at differing frequencies, ie 0.05 Nyquist is coherent with 0.06 Nyquist. The slope $\frac{2}{3}$ of the zone is expected from the $\frac{0.050}{0.075}$ relationship between the two sweeps. In comparison, standard "single-frequency" coherence shows very little similarity between these two signals even though they are simply frequency shifted versions of one another. The off-diagonal coherence indicates that these two signals are jointly non-stationary.

Harmonics, which are correlated between frequencies, also show clearly. Figure 3 shows the same sweep signal but with a harmonic added:

$$f(t) = 50\sin(2\pi t(f_a + \frac{(f_b - f_a)t}{600})) + 50\sin((2.5)2\pi t(f_a + \frac{(f_b - f_a)t}{600})) \quad (9)$$

for $f_a = 0.0$ and $0 \leq t \leq 600$. The harmonics appear as two off-diagonal lines indicating that a given frequency is coherent with itself and another frequency. The angle between the two lines corresponds to the ratio between the frequency content of the signals.

To test the method on real data, we calculated the auto-coherence of a large teleseismic earthquake recorded by a broadband seismic station in Central Asia (AAK) (*Mellors*, 1995). Figure 4 shows the coherence and phase plots. In general, the plots resemble the plots of the sweep function but considerable off-diagonal terms are present, indicating significant correlation between different frequencies. The amount of correlation between different frequencies increases as the frequency increases. The off-diagonal structure also resembles the structure observed in Figure 3. This suggests that the off-

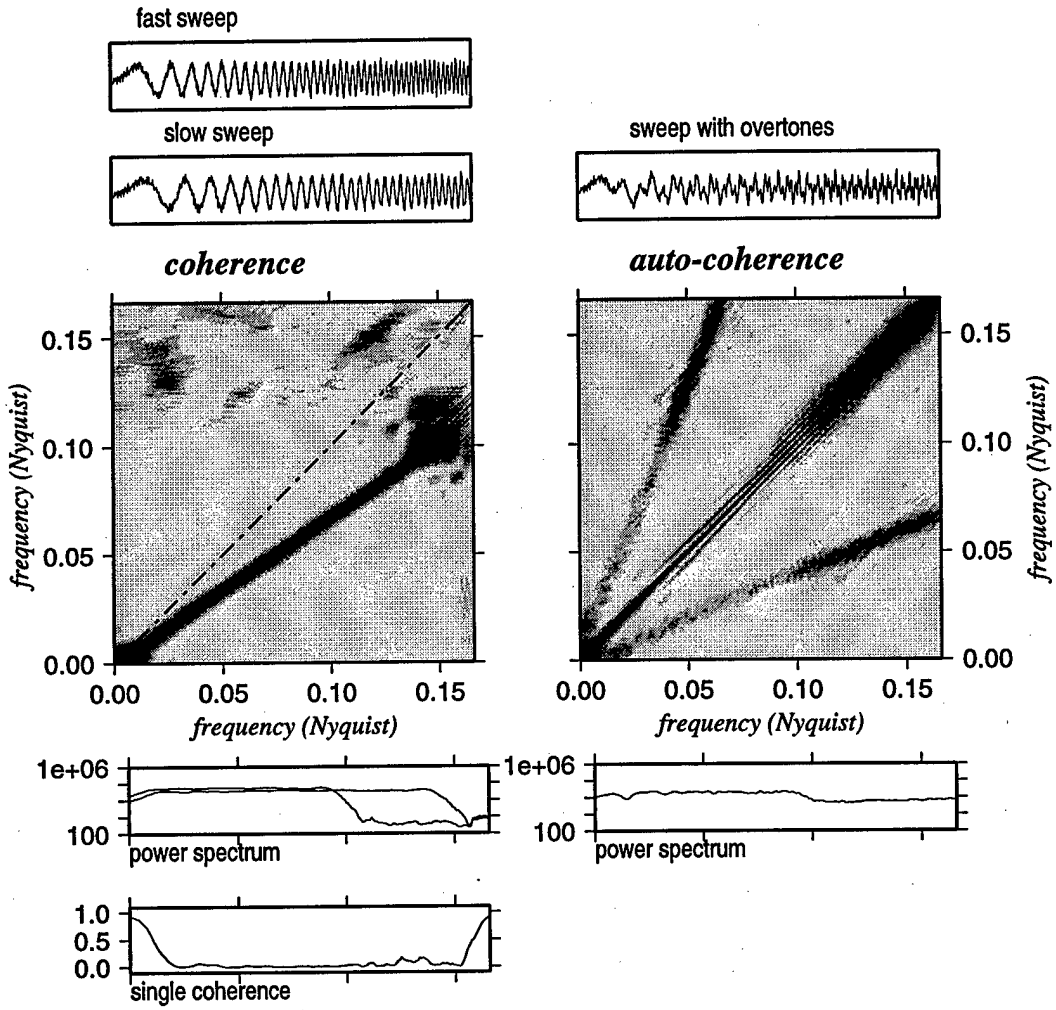

Figure 3: (left) Dual-frequency coherence between two different signals: a fast sweep and a slow sweep. The slope of the zone of high coherence corresponds to the ratio between the frequency content of the signals. The dashed diagonal line is added for reference. For comparison, a plot of the single (standard) coherence between the two sweeps is shown at bottom left. This plot clearly illustrates the advantage of dual-coherence over standard single coherence in identifying frequency dependencies in different signals. (right) Dual-coherence of a signal with higher-frequencies added (as might be produced by multi-pathing). Note the clear off-diagonal terms indicating correlation between frequencies.

diagonal structure may be due to multipathing. Surface waves which have traveled a slightly different path will have slightly different dispersion than the initial path. The multipathing increases with frequency.

The phase plot of the same signal also shows a smooth increase in the region of high coherence. Integrating this will yield the relative phase function of the signal, as the constant phase term is lost.

In large data sets, it is easier to use a time-frequency representation. Formally, *Thomson* (1994) showed that one can express the usual time-frequency spectrogram as a one-dimensional Fourier transform of the dual-frequency spectra taken perpendicular to the $f_1 = f_2$ diagonal. Computationally, it is easier to compute the spectra on different time blocks. For dispersive signals, much of the useful information lies in the frequency combinations very near the main diagonal so we calculate coherency only for frequencies separated by the Rayleigh resolution rather than every possible combination of frequencies. This both speeds the computation and increases the ease of presentation with large data sets. The coherence is calculated for a set of running windows over the entire data set. However, features such as harmonics which will show a high correlation in non-adjacent frequencies will not be evident. To display these as a function of time, it is necessary to identify the specific frequency combinations from the full coherence matrix (such as Figure 3) and plot those. Figure 5 shows a series of sweep signals buried in increasing amounts of noise. Each signal is 600 points long with a 1200 point gap between signals. The auto-coherency is calculated over a series of

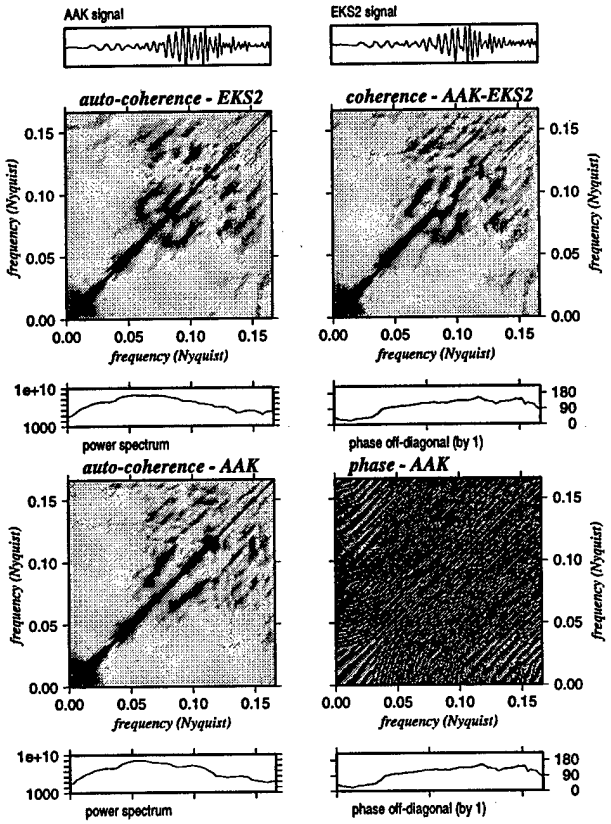

Figure 4: (top) Dual-frequency coherence plots for a large teleseism 40 degree away as recorded by the stations AAK and EKS2 in Kyrgzystan. The seismogram is 1200 seconds long and has been decimated to 0.8 sps. Seismometer response is broadband. The individual dual-frequency dual coherence plots are shown for both stations and the cross-coherence between the stations is shown at the upper left. Note the asymmetry of the plot showing coherence between AAK and EKS2. The off-diagonal terms in the auto-coherence plots demonstrates that the signals are non-stationary.

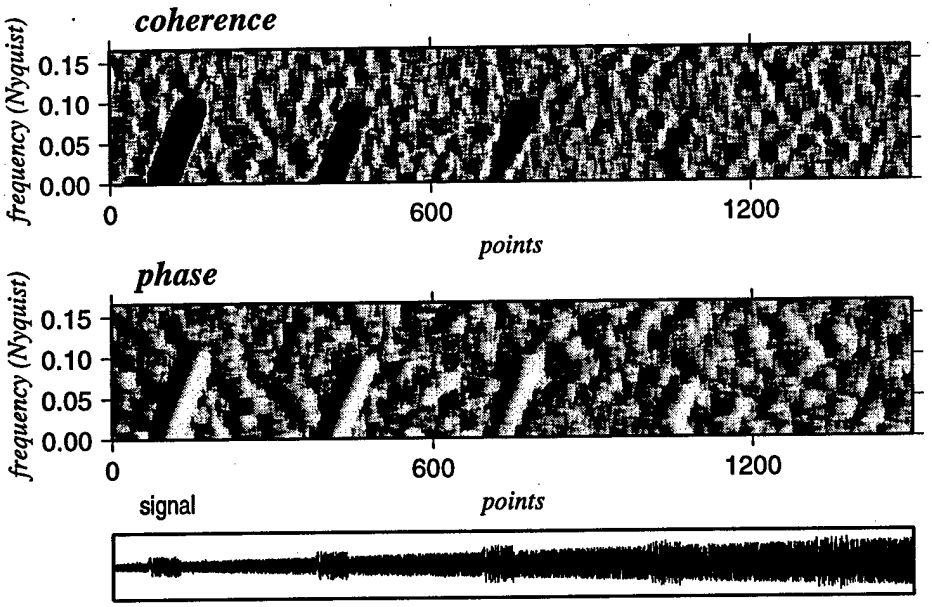

Figure 5: Coherence as a function of time and frequency for a synthetic signal consisting of a sweep buried in increasing white noise. The coherence is calculated over a series of overlapping windows which are averaged together. This plot is similar to a sonogram but displays coherence rather than spectral amplitude. The coherence between adjacent frequencies only is plotted rather than all possible frequency combinations.

600 point running windows. We see that the coherent signal is immediately obvious and that the change in frequency (lower to higher) is also obvious.

Figure 6 shows a similar auto-coherency/time/frequency plot for two seismograms of events recorded by station AAK in Kyrgyzstan. The top shows the same large earthquake as in Figure 4 and the bottom shows a smaller, regional event. The surface waves of the large event are obvious, as well as the body phases. The lower seismogram is a smaller regional event. Al-

though the event has a low signal-to-noise and is difficult to see in the raw time series, it is clearly apparent in the coherence plot. Only with filtering is the seismogram easily visible in the time series plot. This suggest that dual coherence may be an effective method to detect small events as well as to identify phases and features in the seismograms.

Finally, the signal can be filtered to enhance the coherent frequencies. After calculating the coherence, we rebuild the signal keeping only the coherent frequencies and rejecting frequencies with low coherence. Since noise is generally non-coherent and dispersive surface waves are very coherent, this is a powerful way to extract the useful signal from noise. We must choose a specific combination of frequencies to define the coherence and we again use adjacent frequencies.

The procedure is straightforward. We calculate the coherence in the frequency domain over a series of overlapping windows, and then convert the signal back into the time domain, keeping only the frequencies that possess a coherence above a certain threshold. The resulting signal then only contains coherent energy. However, samples less than one window length from the end will have less overlapping than the rest of the signal.

We tested the procedure on the same repeated sweep signal in noise as before. A window length of 600 points was used with the time windows overlapping by 10, so that each point in the interior is the average of 60 windows. A range of cutoff coherence thresholds were tested. A threshold of 0.5 rejects all frequencies whose coherence with the neighboring frequency

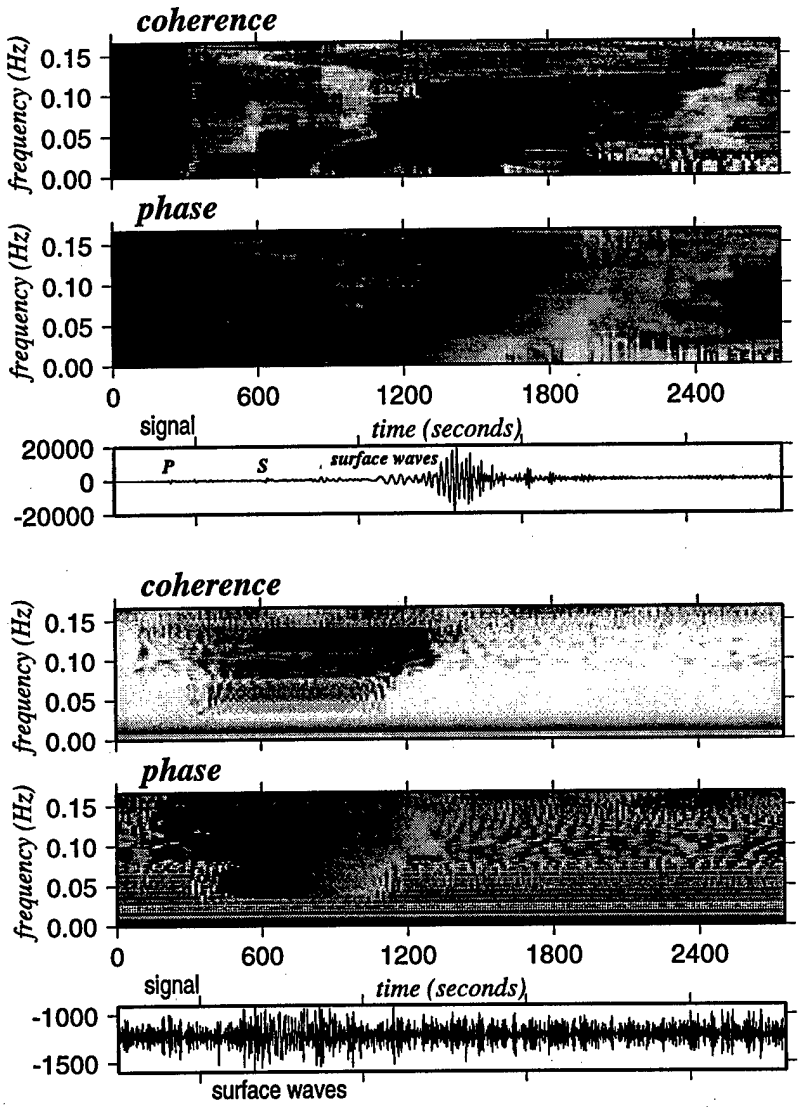

Figure 6: (top) Coherence/time plots for a large teleseism recorded by station AAK in Kyrgyzstan. The surface waves show a clear signature on both the coherence and phase plots. The body waves also show distinctly on the phase plot.(bottom) Coherence/time plot for a magnitude 4 event 15 degrees away in Western China as recorded at station AAK in Kyrgyzstan. The surface waves are difficult to see in the raw data but are obvious in the coherence plot.

is less than 0.5. A threshold of 0.0 retains all frequencies and reproduces the original signal except for the one window length edge effects referred to above. A threshold of 1.0 removes all frequencies and produces a zero signal (we weight the first frequency to zero).

The results (Figure 7) are good. Using a cutoff of 0.8, the noise is mostly removed but the signal remains. Noise within one window length of the signal that lies within the band of coherent energy is retained, causing a smearing of the signal. Note that it is impossible to extract the signal with a band-pass filter as both the noise and the signal are broadband. The reproduction of the signal is not perfect, as the amplitude spectra of coherent signals is affected by noise lying within the coherent band. With higher noise levels (Figure 7), the signal can still be recovered but the distortion of the recovered signal increases. The amount of increase in the signal-to-noise ratio depends on a number of factors including window length, amount of offset, and cutoff threshold, all of which depend on characteristics such as sample rate and noise level and therefore should be tuned for a particular data set. Two important features should be noted; one, an average stationary signal, which is incoherent at different frequencies, is greatly reduced and two, this filter requires no *a priori* knowledge of the signal.

5 Conclusions

We have shown that dual-frequency coherence is an effective method of analyzing signals. Although we have shown only seismic data, we believe that it

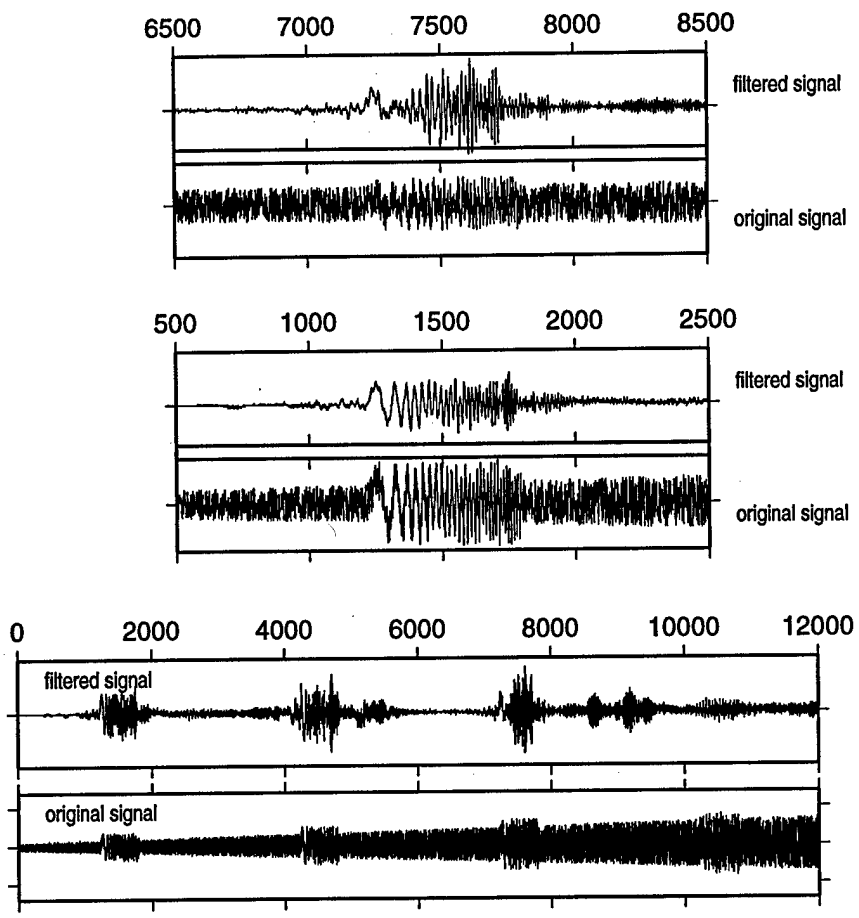

Figure 7: Dual-coherency filtering of the repeated sweep in noise waveform shown in Figure 5. The original signal and a filtered version is shown at the bottom. Close-ups of the individual sweeps are shown in low noise and high noise backgrounds. The coherency threshold was set at 0.75, so all frequencies with a coherence to a frequency one Rayleigh resolution frequency of less than 0.75 were removed.

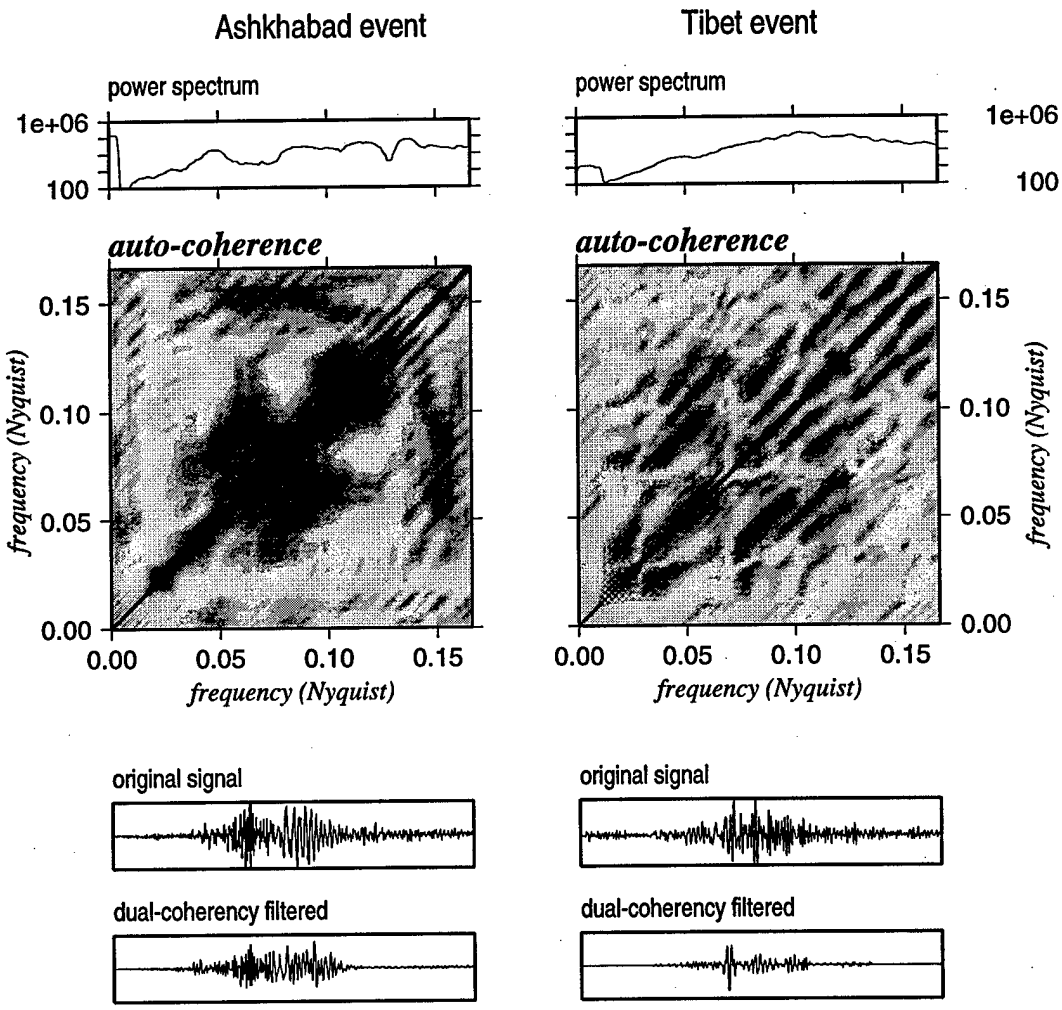

Figure 8: Dual-coherency filtering of two events with differing amounts of multi-pathing. The Tibet event (right) is highly multi-pathed (Pavlis and Mahdi,1993) while the Ashkhabad event (left) shows little multi-pathing. At the top is the time series of the two earthquakes and the full dual-frequency coherence matrix. At the bottom we show unfiltered and coherency filtered versions of the same seismograms. Note the coherency filtered seismogram resembles the original version while the coherency filtered multi-pathed event has been degraded greatly.

may possess a wide range of applications. In the following section we present some possible applications with selected examples.

Signal detection. The coherency filter shows promise as a regional seismic event detection algorithm. For small shallow events at regional distances, the surface waves are the largest part of the wavetrain and that is exactly the section of the waveform that dual-frequency coherence is most suited for detection. In addition, it is possible to simultaneously detect and characterize a signal. The major difficulty has been that microseisms are also coherent over a small frequency band, so for small events the seismograms tend to be dominated by microseismic signals. We plan to test adaptive version of the code which will first tune over sections of data with only noise and selectively eliminate the frequencies with coherent "noise" such as microseisms.

Signal characterization. As shown in Figure 2, estimates of phase relationships can be made from the dual coherence measurements. The ability of dual-frequency coherence to identify harmonic-like signals and signals with frequency translations suggest that it may be an effective method of identifying surface wave multi-pathing, as the surface wave packets arriving from the same source but with slightly different paths will show differing dispersion. We test this idea by using two events that were previously shown to be multi-pathed on the basis of array studies (*Pavlis and Mahdi, 1993*). Figure 8 show these two events. The Ashkhabad event has very little multipathing, according to *Pavlis and Mahdi* (1993), which is expected as its path was largely across relatively undisturbed platform. The Tibet event showed a

high degree of multi-pathing as it traveled through several different terrains (Tarim Basin and Tien Shan). The coherency filter results reflect this. The single-path event shows a single relatively high amplitude wavetrain, indicating that the waveform was smoothly coherent across a range of frequencies. The multi-pathed event shows a much more ragged set of waveforms indicating that the wavetrain is not extremely coherent. The non-coherent arrivals due to the interfering wave packets have been largely filtered out.

Waveform comparison. Dual-frequency coherence also offers an easy method of comparing two signals, especially ones that may be fairly similar. Small frequency and phase shifts will be readily apparent. With a time/coherence plot, it is simple to test exactly which sections of the signal show a misfit, in both the frequency and time domains.

Filtering. The filtering shown in this paper represents the simplest version. More elaborate versions, using variable weighting for example, should give even better performance.

The other important point of this paper is that the surface wave seismograms appear to have significant non-stationary component. This has important implications for any surface wave analysis that depends on techniques that assume stationarity of the signals.

6 References

Bloomfield, P., 1976. *Fourier analysis of time series: An introduction.* Spectral analysis for physical applications, John Wiley & Son.

Foster, M. R. and N. J. Guinzy, 1967. The coefficient of coherence: its estimation and use in geophysical data processing. *Geophysics*, **XXXII**, 603-617.

Hinich, M. J. and C. S. Clay, 1968. The application of the discrete Fourier transform in the estimation of power spectra, coherence, and bispectra of geophysical data. *Revs. of Geophys.*, **6**, 347-363.

Hough, S. E. and E. H. Field, 1996. On the coherence of ground motion in the San Fernando Valley. *Bull. Seis. Soc. Amer.*, **86**, 1724-1732.

Kuo, C., C. R. Lindberg, and D. J. Thomson, 1990. Coherence established between atmospheric carbon dioxide and global temperature. *Nature*, **343**, 395-400.

Lanzerotti, L. J., D. J. Thomson, A. Meloni, L. V. Medford, and C. G. Maclennan, 1986. Electromagnetic study of the Atlantic margin using a section of the transatlantic cable. *J. Geophys. Res.*, **91**, 7417-7427.

Lòeve, M., 1945. Analyse harmonique gènèrale d'une fonction alèatoire. *Comptes. Rendus. Acad. Des. Sci.*, **220**, 380-382.

Lòeve, M., 1963. *Probability Theory.* Van Nostrand, Princeton, N.J..

Matlab, 1994. *Version 4.2c.* The MathWorks, Inc, Natick, MA.

Mellors, R. J., 1995. *Two studies in Central Asian seismology: A teleseismic study of the Pamir/Hindu Kush seismic zone and analysis of data from the Kyrgyzstan broadband seismic network.* Indiana University, Bloomington, Indiana.

Mellors, R. J., F. Vernon, and D. Thomson, 1996. Detection of dispersive signals using multi-taper dual-frequency coherence. In "*Proceedings of the 18th Seismic Research Symposium on Monitoring a Comprehensive Test Ban Treaty*", ed. J. F. Lewkowicx, J. M. McPhetres, and D. T. Reiter, Annapolis, Maryland, pp. 745-753.

Park, J. J., F. L. Vernon III, and C. R. Lindberg, 1987. Multitaper spectral analysis of high-frequency seismograms. *J. Geophys. Res.*, **92**, 12,675-12,684.

Park, J, S. L. D'Hondt, J. W. King, and C. Gibson, 1993. Late Cretaceous precessional cycles in double time: a warm-earth Milankovitch response. *Science*, **261**, 1431-1434.

Pavlis, G. and H. Mahdi, 1993. Surface wave propagation in central Asia: Observations of scattering and multipathing with the Kyrgyzstan broadband array. *J. of Geophys. Res.*, **101**, 8437-8455.

Percival, D. B. and A. T. Walden, 1993. *Spectral analysis for physical applications.* Cambridge Univ. Press, Cambridge.

Priestley, M. B., 1981. *Spectral analysis and time series.* Academic Press, San Diego, CA.

Slepian, D., 1978. Prolate spheroidal wave functions, Fourier analysis, and uncertainty-V: The discrete case. *Bell Syst. Tech. J.*, **57**, 1371-1429.

Slepian, D., 1983. Some comments on Fourier analysis, uncertainty, and modeling. *SIAM rev.*, **25**, 379-393.

Thomson, D. J., 1982. Spectrum estimation and harmonic analysis. *IEEE Proc.*, **70**, 1055-1096.

Thomson, D. J., 1994. An overview of multiple-window and quadratic-inverse spectral estimation methods. *ICASSP Proc.*, **6**, 73-76.

Thomson, D. J., 1993. Non-stationary fluctuations in "stationary" time series. *Proc. SPIE*, **2027**, 236-244.

Thomson, D. J., and A. D. Chave, 1991. Jack-knifed error estimates for spectra, coherences, and transfer functions. In "*Advances in spectrum analysis and array processing:1*", ed. S. Haykin, Prentice Hall, pp. 58-113.

Tick, L. J., 1966. Estimation of coherence. In "*Spectral Analysis of Time Series*", ed. , John Wiley, New York, pp. 133-152.

Vernon, F., R. J. Mellors, and D. Thomson, 1995. Broadband signal enhancement of seismic array data: application to long-period surface waves and high-frequency wavefields. In "*Proceedings of the 17th Seismic Research Symposium on Monitoring a Comprehensive Test Ban Treaty*", ed. J. F. Lewkowicx, J. M. McPhetres, and D. T. Reiter, Scottsdale, Arizona, pp. 807-814.

Vernon, F. L., J. B. Fletcher, L. Carroll, A. D. Chave and E. Sembera, 1991. Coherence of seismic body waves from local events as measured by a small-aperture array. *Journal of Geophysical Research, B, Solid Earth and Planets*, **96**, 11,981-11,996.